Automatic Segmentation of Single Neurons Recorded by Wide-Field Imaging Using Frequency Domain Features and Clustering Tree

by

Ruofan Wu

A Thesis Presented in Partial Fulfillment
of the Requirements for the Degree
Master of Science

Approved August 2016 by the
Graduate Supervisory Committee:

Jennie Si, Chair
Rosalind Sadleir
Sharon Crook

ARIZONA STATE UNIVERSITY

December 2016

ABSTRACT

Recent new experiments showed that wide-field imaging at millimeter scale is capable of recording hundreds of neurons in behaving mice brain. Monitoring hundreds of individual neurons at a high frame rate provides a promising tool for discovering spatiotemporal features of large neural networks. However, processing the massive data sets is impossible without automated procedures. Thus, this thesis aims at developing a new tool to automatically segment and track individual neuron cells. The new method used in this study employs two major ideas including feature extraction based on power spectral density of single neuron temporal activity and clustering tree to separate overlapping cells. To address issues associated with high-resolution imaging of a large recording area, focused areas and out-of-focus areas were analyzed separately. A static segmentation with a fixed PSD thresholding method is applied to within focus visual field. A dynamic segmentation by comparing maximum PSD with surrounding pixels is applied to out-of-focus area. Both approaches helped remove irrelevant pixels in the background. After detection of potential single cells, some of which appeared in groups due to overlapping cells in the image, a hierarchical clustering algorithm is applied to separate them. The hierarchical clustering uses correlation coefficient as a distance measurement to group similar pixels into single cells. As such, overlapping cells can be separated. We tested the entire algorithm using two real recordings with the respective truth carefully determined by manual inspections. The results show high accuracy on tested datasets while false positive error is controlled within an acceptable range. Furthermore, results indicate robustness of the algorithm when applied to different image sequences.

DEDICATION

To my parents

ACKNOWLEDGMENTS

Foremost, I would like to express my sincere gratitude to my MS thesis advisor Professor Jennie Si for her continuous support of my MS studies and research, for her patience, motivation, enthusiasm, and immense knowledge. Her encouragement, insightful comments and guidance helped me throughout the course of the research and writing of this thesis. I would also like to thank Simon Shen for his contribution on building ground truth for testing. I take this opportunity to express my gratitude to my committee members, Dr. Rosalind Sadleir and Dr. Sharon Crook, for their insightful comments. I also thank Dr. Xue Han, Dr. Hua-an Tseng, Kyle Hansen and other lab members for introducing the challenging problem to me and for providing continuous support to my research.

TABLE OF CONTENTS

Page

LIST OF TABLES

Table Page

LIST OF FIGURES

CHAPTER 1

INTRODUCTION

Fluorescent imaging is a promising tool for extracellular recording of neuronal activity. It is capable of providing high resolution recording both spatially and temporally as rapidly responsive fluorescent protein and optical imaging technology improves (Chen et al., 2013; Sun et al., 2013). As a result, two photon imaging is becoming very popular in neuroscience field since laser excitation greatly reduces background noise and bring an ultra-high spatial resolution. However, the laser scanning mechanism also limits its frame rate to about 4 frames/second due to its mechanical limitation (Tian et al., 2009). Wide-field imaging is another useful technique of fluorescent imaging (Mohammed, Gritton, Tseng, Bucklin, & Yao, 2016). The use of LED excitation makes high frame rate recording possible. However, high recording rate requires short exposure time and fast shutter speed of the camera, which usually lowers the signal to noise ratio. Also, imaging quality can be affected by light shadows since the wavelength of the light source is in the visible light range, which brings significant challenges to cell segmentation.

Cell segmentation techniques have been developed for imaging studies of biological systems in laboratory studies of blood cells, lymphocytes cells and stem cells (Liu, Jurrus, Seyedhosseini, Ellisman, & Tasdizen, 2012)(Meijering, 2012). Most of the algorithms, for example the watershed algorithm, are histogram and morphology based, which rely on intensity thresholding. These algorithms perform well for images with uniform background. In reality, due to physical limitations such as focus area and light scattering, wide-field imaging rarely provides a uniform background.

Overlapping cells in an image is a very common problem in wide-field imaging even though it is a non-issue for two photon imaging because of its limited imaging area. However, wide-field imaging records hundreds of cells in each frame during each recording session and a significant portion of an image frame contains overlapping cells. Feature detection is a popular approach to solving the overlapping cell segmentation problem, which uses a filter template. But it assumes that the shape of a cell is invariant. Trace clustering is another solution for overlapping segmentation. Previous research showed that k-means clustering could be used in this case (Wu & Barbat, 1996).

As shown in the above, uniform illuminance condition, uniform and invariant cell shape are usually assumed when segmenting individual neuron cells recorded by wide-field imaging even though these conditions rarely hold true (Wu & Barbat, 1996). Therefore, this thesis provides a new method for neuron segmentation based on wide-field imaging to directly address unstable background and cell overlapping issues. This method uses frequency domain features for detection and clustering tree for individual cell identification.

CHAPTER 2

ALGORITHM

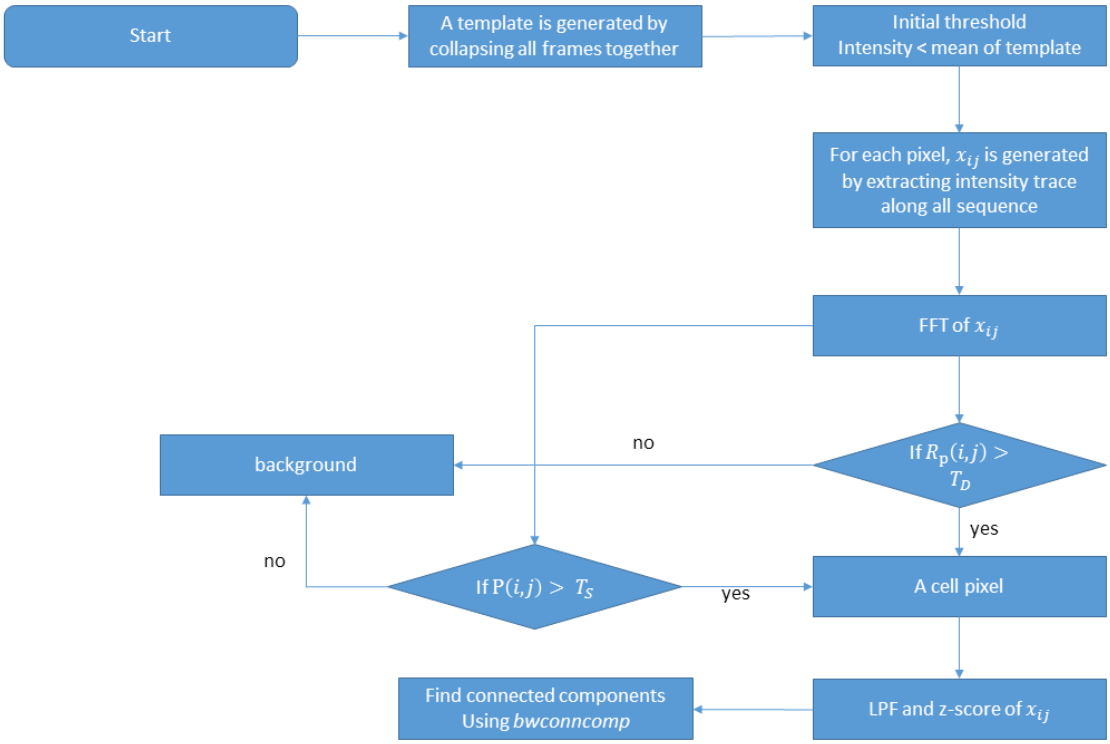

Figure 1. Flow Chart of Algorithm

Image preprocessing

The raw image sequence was recorded and stored in TIFF format (Mohammed et al., 2016). Each file contains 2,048 frames with a 1,024×1,024 pixel resolution. Image registration is first performed to compensate for frame movement due to physical movement of the animal caused by respiration, blood flow, and muscle movement. Motion correction has been proven necessary to reduce these motion artifacts. Previous research (Mohammed et al., 2016) has provided a reliable solution to this problem. An artificially created frame, named maximum image frame, is first obtained by collapsing

all image frames together with each pixel represented by the largest intensity value for each pixel.

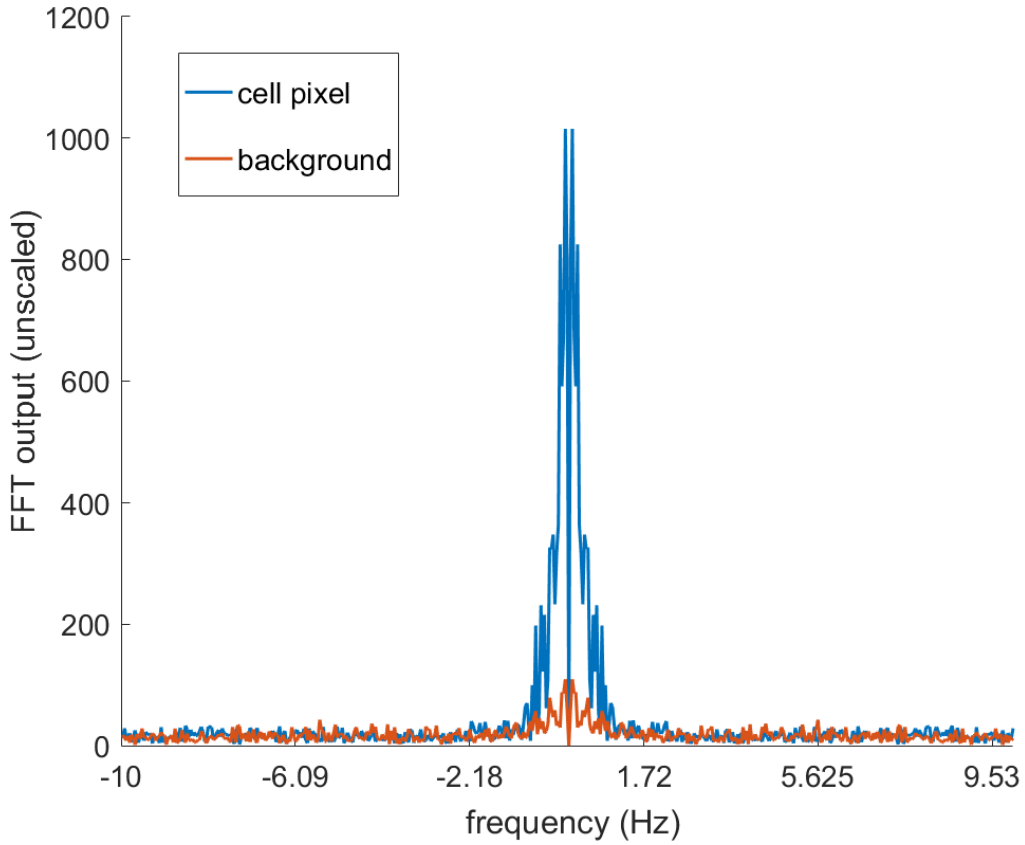

Figure 2. Power Spectral Density of Background and Cell

Segmentation

	Definition
$\boldsymbol{i,j}$	Coordinates of a pixel
$\boldsymbol{x_{i,j}}$	A trace or a vector of intensity values of pixel $(\boldsymbol{i,j})$
$\boldsymbol{T_S}$	Threshold for static segmentation
$\boldsymbol{T_D}$	Threshold for dynamic segmentation
$\boldsymbol{P(i,j)}$	Maximum power spectral density of the intensity trace of a pixel at $(\boldsymbol{i,j})$
$\boldsymbol{\bar{P}(i,j)}$	Mean of $\boldsymbol{P(m,n)}$ where $\boldsymbol{m = [\mathrm{i}-10, \mathrm{i}+10]}$, $\boldsymbol{n = [\mathrm{j}-10,\ \mathrm{j}+10]}$
$\boldsymbol{R_p(i,j)}$	A pixel power ratio calculated by $\frac{\boldsymbol{P(i,j)}}{\boldsymbol{\bar{P}(i,j)}}$, used for dynamic segmentation thresholding
$\boldsymbol{T_C}$	Cut-off value for adaptive clustering tree
$\boldsymbol{B_u, B_l}$	Lower bound $\boldsymbol{B_l}$ and upper bound $\boldsymbol{B_u}$ for cell size, respectively

Table 1. List of Variables

Since image pixel background intensity varies sequence by sequence, a simple intensity thresholding does not provide sufficient segmentation of all cells from different background conditions. Therefore, activities in a full sequence would be a better measurement when performing segmentation. To achieve this, an intensity trace $x_{i,j}$ is extracted for each pixel along the entire sequence. Then fast Fourier transform was performed on each pixel trace to obtain their frequency spectrum. As Figure 2 shows, a background pixel presumably carries noise information and therefore, its spectrum

distribution is a typical white noise. In contrast, a neuron cell pixel would fire several times during a recording session so that its power spectrum exhibits a peak in a certain low frequency range. By using this property represented in power spectrum density (PSD) of an image trace, cell pixels can be segmented.

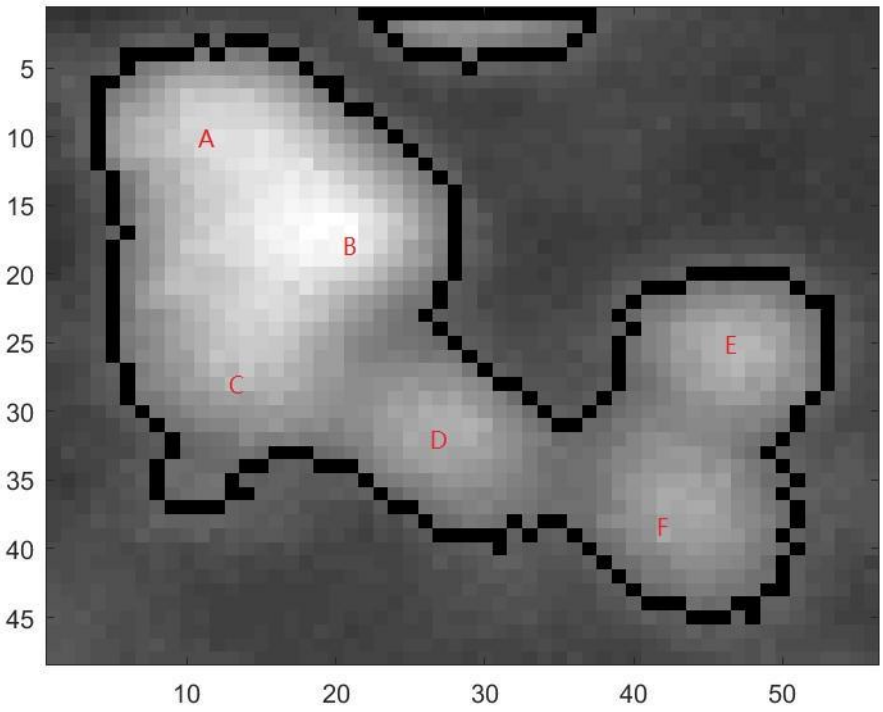

Figure 3. A Typical Connected Cell Area

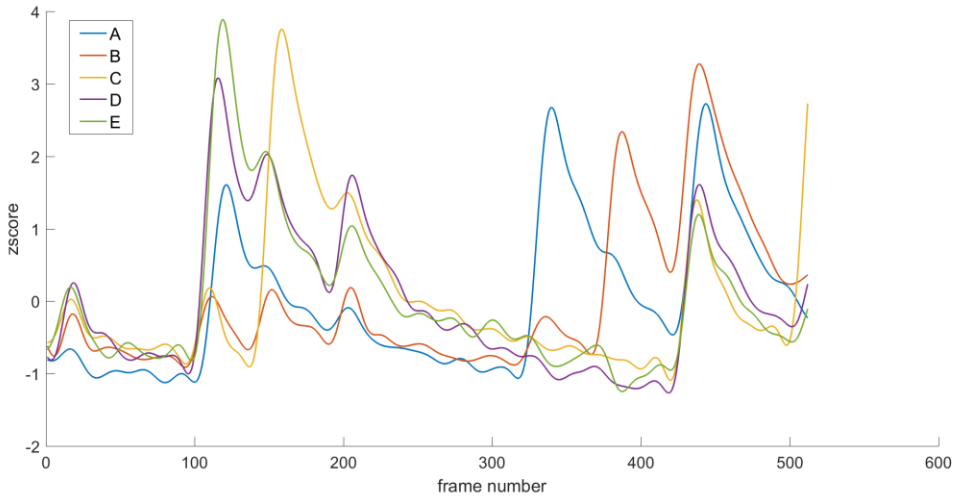

Figure 4. Signal After Filtering and Normalization Shows Different Firing Patterns that Can be Used for Clustering

Another problem is caused by high power magnification during imaging and thus some areas of an image frame goes out of focus. This is quite visible in an image frame. This also conceals the illuminance of a cell near the edge of the out-of-focus area. Meanwhile, the brain surface is slightly curved, and thus the imaging area is not placed flat on the same plane. The recording cannula usually can't touch the imaging plane tightly in this case. Out-of-focus area is typically associated with blurred cells and darker than those cells in the imaging plane. This makes it difficult to detect by the above algorithm.

$$\boldsymbol{R_p(i,j)} = \frac{\boldsymbol{P(i,j)}}{\boldsymbol{\overline{P}(i,j)}} \qquad (1)$$

Thus, a dynamic process was introduced. A pixel power ratio $\boldsymbol{R_p(i,j)}$ which is defined as the ratio between $\boldsymbol{P(i,j)}$ and $\boldsymbol{\overline{P}(i,j)}$ is calculated in Equation (1). If $\boldsymbol{R_p(i,j)}$ is higher than the threshold T_D, the pixel will be counted as a cell pixel. This dynamic process can properly identify out-of-focus cell even if they don't have enough intensity change. However, high density of cell in focus area will limit its performance because so many

cells exist within a10 pixels range which significantly raise the average spectral power. Therefore, this two processes will work in parallel and complement each other. PSD thresholding is responsible for areas in focus and dynamic process take care of the pixels out of focus.

After picking out the cell pixels and removing the background pixels, a set of size bound, lower bound B_l and upper bound B_u, is set in order to eliminate isolated noisy spots. Any cell smaller than B_l will be removed. Prior to clustering process, low pass filtering is used to remove high frequency noise and all pixels are properly grouped based on whether they are connected or not. This step will reduce the computing consumption in the following clustering step.

Clustering:

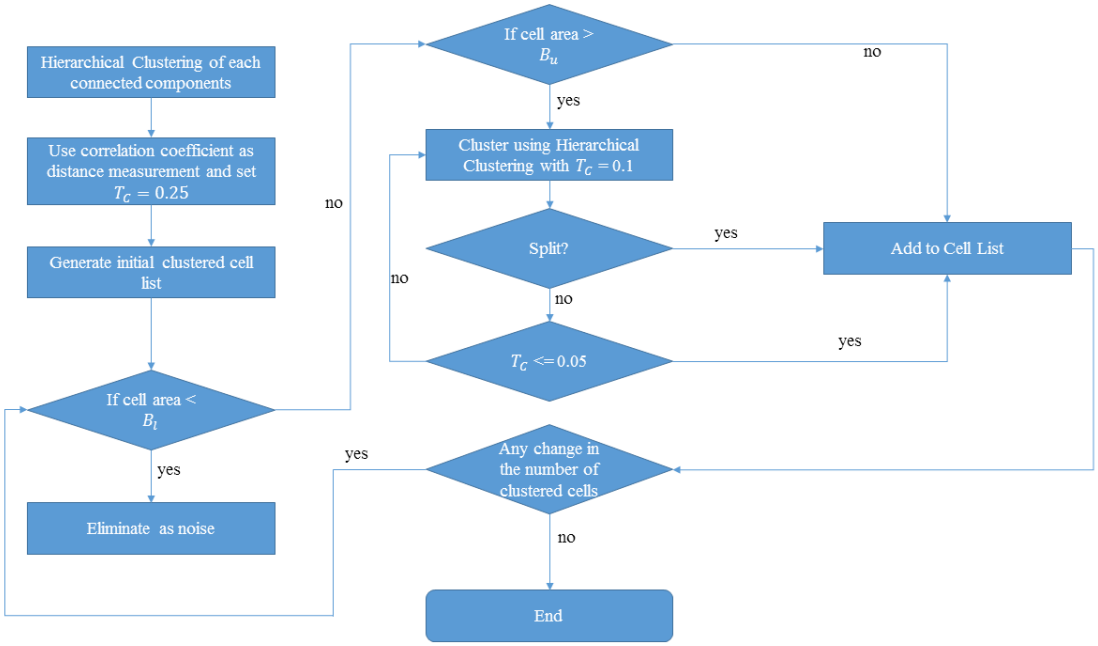

Figure 5. Flow Chart of Clustering

Practically, a single connected area possibly contains a single cell or multiple cells, sometimes even overlapping cells. A clustering process on the z-score of the original

traces was designed to split multiple (overlapping) cells. As Figure 4 shows, pixels that belong to the same cell has a similar signal trace while those belong to different cells are quite different. Therefore, we can use the correlation coefficient between two pixel traces as the distance measure for clustering or overlapping cell separation. The hierarchical clustering algorithm was performed by built-in MATLAB function *pdist*, linkage and *clusterdata*.

The initial cutoff value T_C was set as 0.25, which is empirical and determined by trial and error. In principal, this value can be set higher because we use an adaptive T_C in the next step. But higher value results in more computation. So setting initial value as 0.25 is a trade-off between performance and computing cost. The separated cells after initial clustering are defined as candidate cells. A complication can negatively impact the clustering outcome. That is synchronized firing of cells, which was observed in all the sequences, for example, trace E and F in Figure 4. In another word, they present very similar traces and the initial T_C is not able to split them. An adaptive process was introduced to solve this problem. After initial clustering, if the area of a cell is larger than an upper bound B_u, T_C will keep decreasing by 0.01 until the cell being separated or T_C reached 0.05, which is considered as an oversized single cell. Figure 7 shows the result of this adaptive process. Cells E and F are eventually separated after adaptive process. This adaptive process is independent among cell candidates thus each cell candidate will have a unique T_C and become an identified cell.

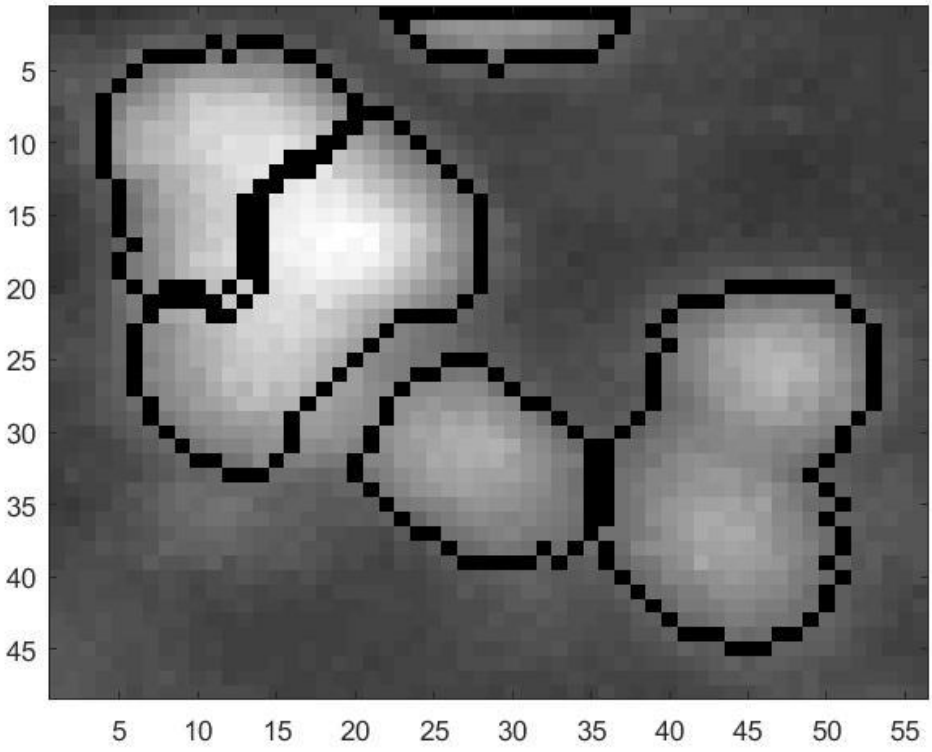

Figure 6. Without Adaptive Cut-off, Most Cells are Isolated. But Cells with Similar Firing Patterns Remain Connected

During this adaptive process, some smaller area will be split off, usually less than 25% of the original cell. Two possible explanations could be made. First, this area belongs to an overlapping area between two cells so it contains signal from both of them. Algorithm will automatically search its neighbor cells and compare correlation coefficient of the two traces. If it reaches a criterion, usually set as 0.6, it will be considered as overlapping area and to be a part of both cells. If not, the second explanation is applied, which considers this area as the shadow of a cell. In this situation, it has a similar trace to the cell body but

actually is not a part of them and will be discarded.

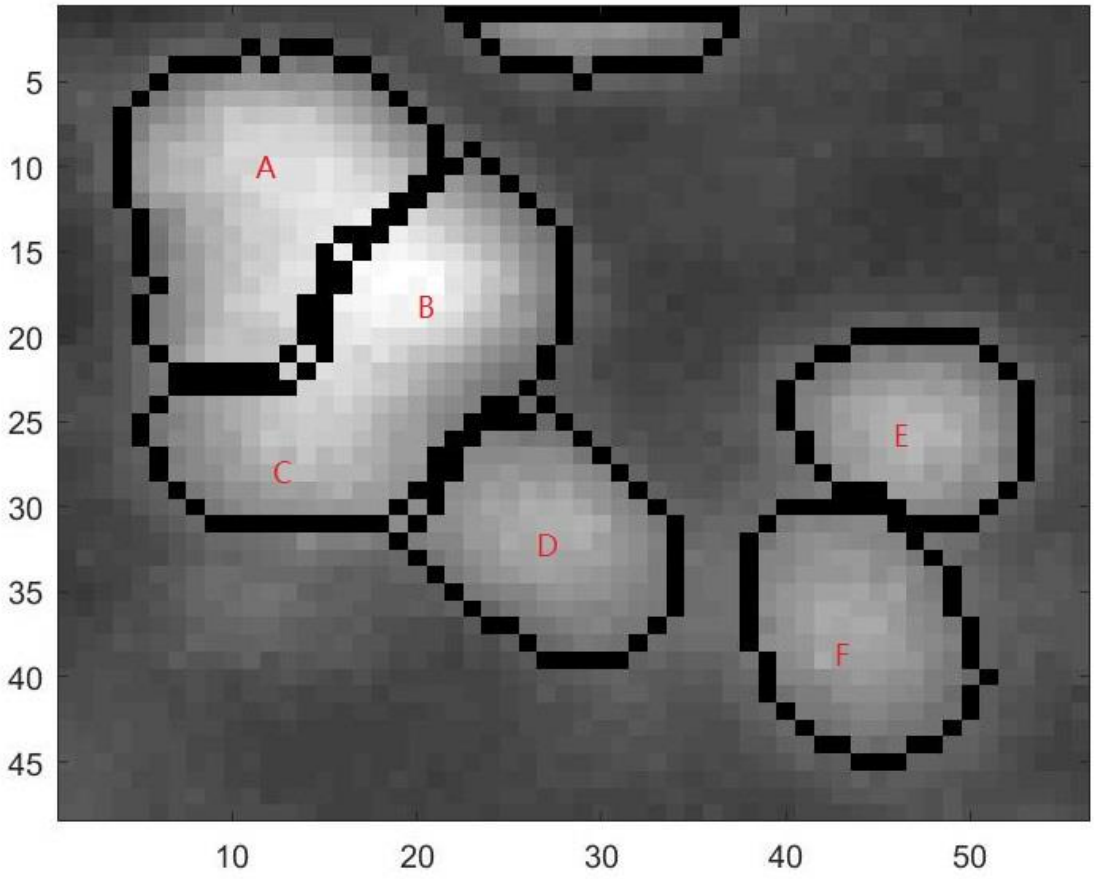

Figure 7. With Adaptive Cut-off, Two Cells Having Similar Firing Patterns are Separated

CHAPTER 3

RESULT

Two datasets were tested in this study. Each has 2,048 frames with 1,024×1,024 pixel resolution and recorded at 20 frames/second. Two experts independently inspected these two datasets to carefully establish the ground truth, which was used for testing. During visual inspection, we found it difficult to identify individual cells in those out-of-focus areas because cells show less activity and the background is darker than the focused area. Besides, cells within the focused areas are possibly covered by the shadow of neighbor cells due to high cell density. Thus, after we manually inspect each possible cell, 731 and 392 cells were positively selected for Ali22 and Ali26 dataset, respectively.

	Definition
False positive	cells detected by algorithm but do not belong to the truth set
False negative	cells that the algorithm missed
True positive	cells successfully detected by algorithm
Sensitivity	true positive / (true positive + false negative)
False negative rate	false negative/ (true positive + false negative)
Accuracy	true positive / (true positive + false positive)
False positive rate	false positive / (true positive + false positive)

Table 2. Definition of Key Terms

Table 2 is a summary of the terms used in this study. Generally, false negative is acceptable when we have already recorded hundreds of cells. But false positives should be controlled as tightly as possible to reduce its adverse impact on further neuron science

study because it may provide erroneous information and therefore interfere with the true neural network under study.

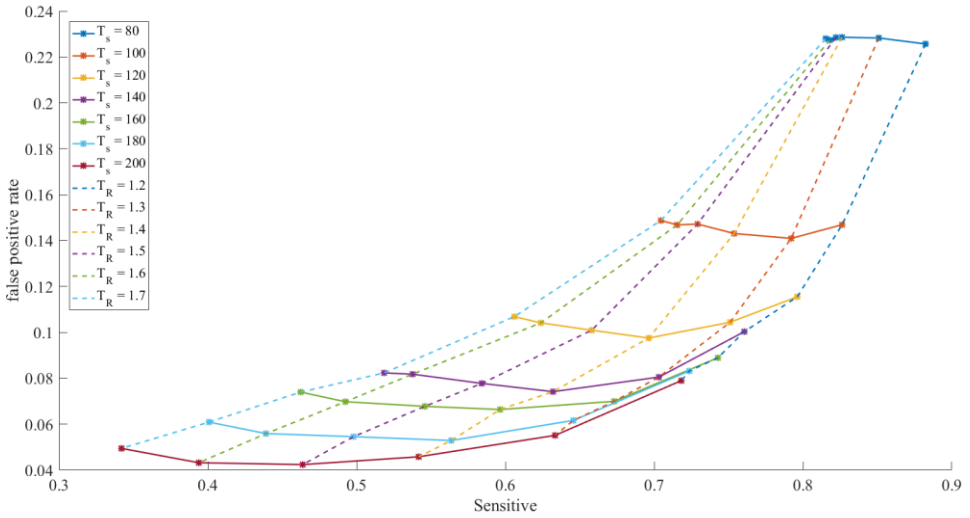

Figure 8. Ali22 Sensitivity vs False Positive Rate

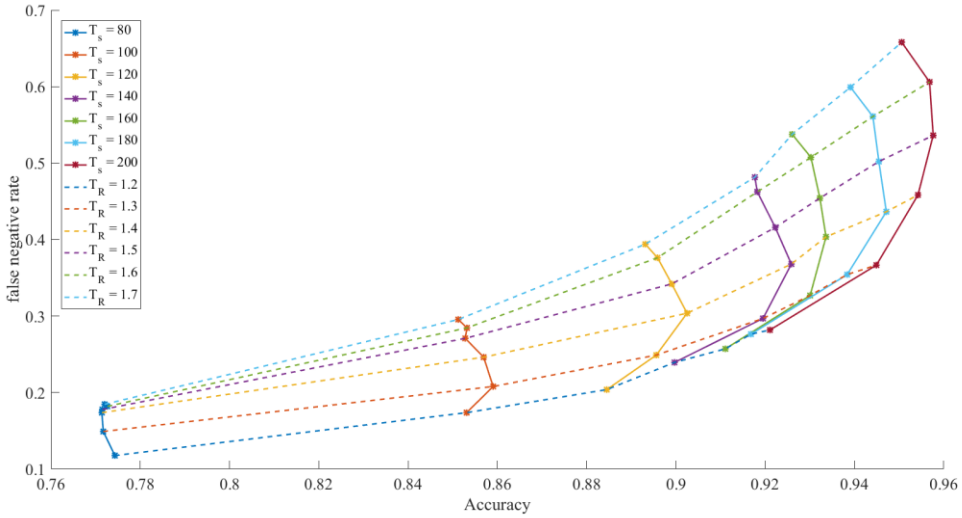

Figure 9. Ali22 Accuracy vs False Negative Rate

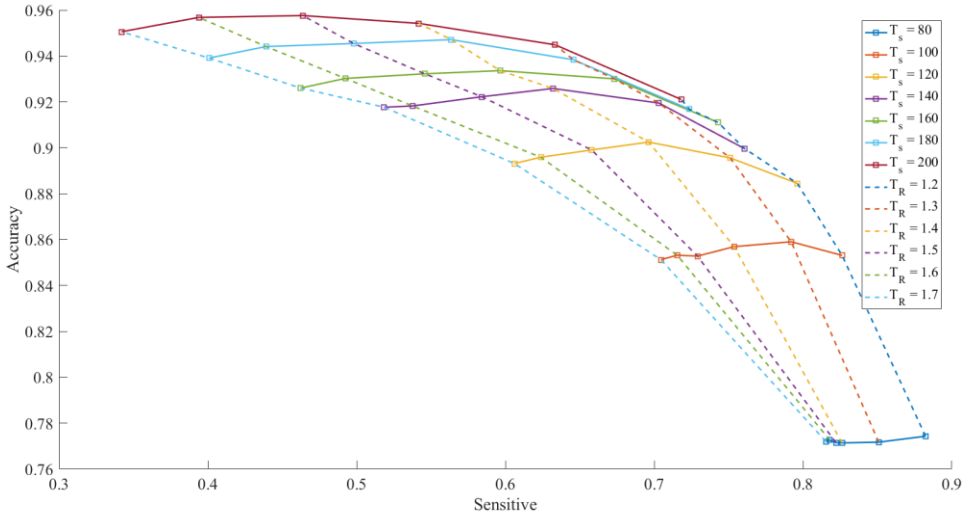

Figure 10. Ali22 Sensitivity vs Accuracy

As Figure 10 shows, accuracy drops if we try to increase the number of identified cells. In Ali22 dataset, Sensitivity can reach above 75% while we maintain accuracy at about 90%, which means a quarter of cells will be missed out if we keep false positive rate low. The explanation of error will be stated in Discussion. Figure 14 shows the result of Ali26 dataset. It has a similar result to Ali22 which can reach about 73% accuracy while keep false positive rate under 10%. But we also can notice that these two data sets show different features. Ali26 has much tighter curves while T_D changes. Thus, dynamic segmentation contributes less than static segmentation in Ali 26 possibly due to cells are more concentrated in central area rather than out-of-focus area.

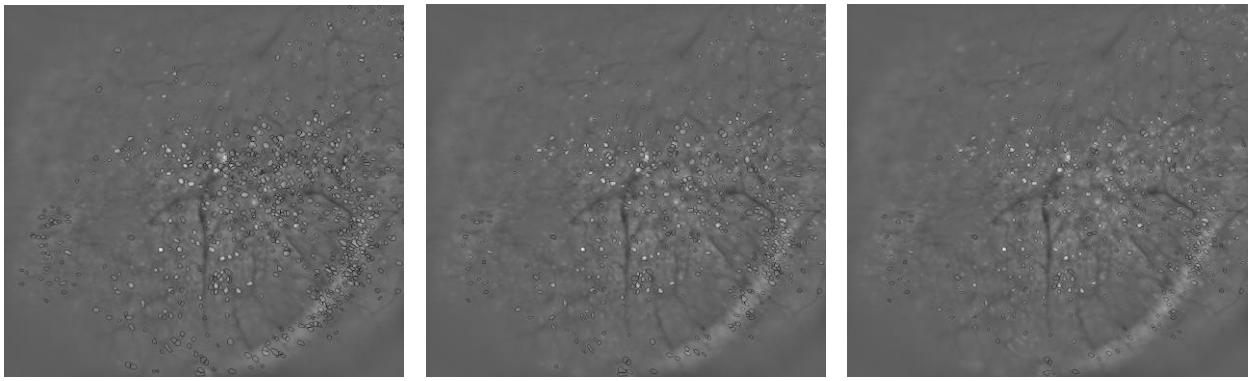

Figure 11. Ali22 Output: Parameter from Left to Right (T_s = 80, T_D= 1.4; T_s = 120, T_D =1.5; T_s= 160, T_D= 1.5)

Figure 11 shows how the segmentation results change if some key parameters change in the segmentation algorithm. T_s controls the PSD threshold in static segmentation while T_D controls dynamic segmentation. Although two segmentation processes were simply overlapped to obtain the final segmentation result, it is obviously that two parameters take charge in the focused area and out-of-focus area independently. Static segmentation is more efficient in the focused area since it focuses on absolute PSD level while dynamic segmentation is influenced by high density cell activities. In out-of-focus area, conversely, dynamic segmentation is dominant because of its high sensitivity on sparse low PSD cell.

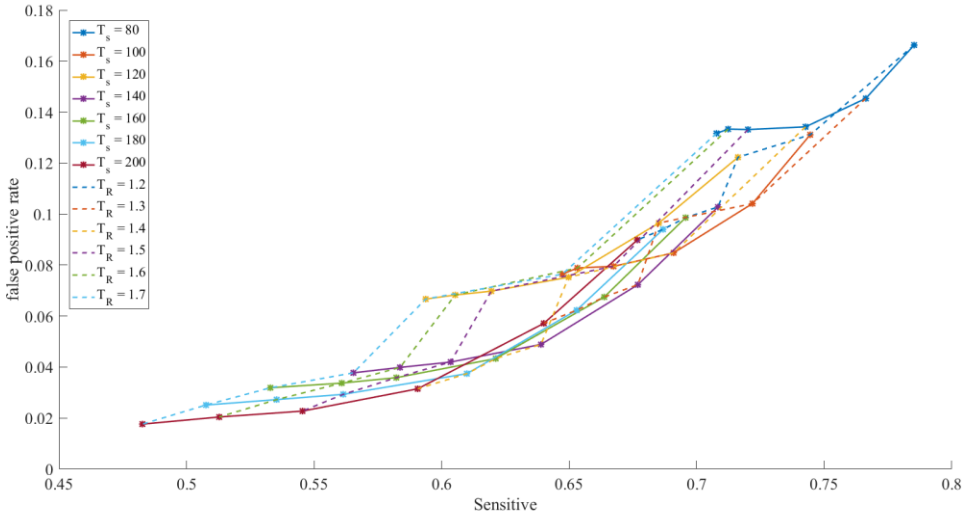

Figure 12. Ali26 Sensitivity vs False Positive Rate

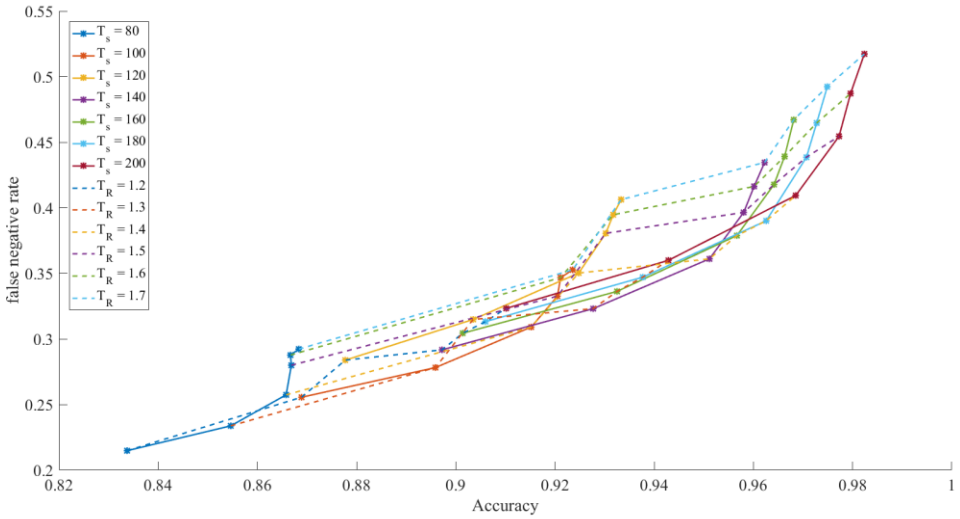

Figure 13 Ali26 Accuracy vs False Negative Rate

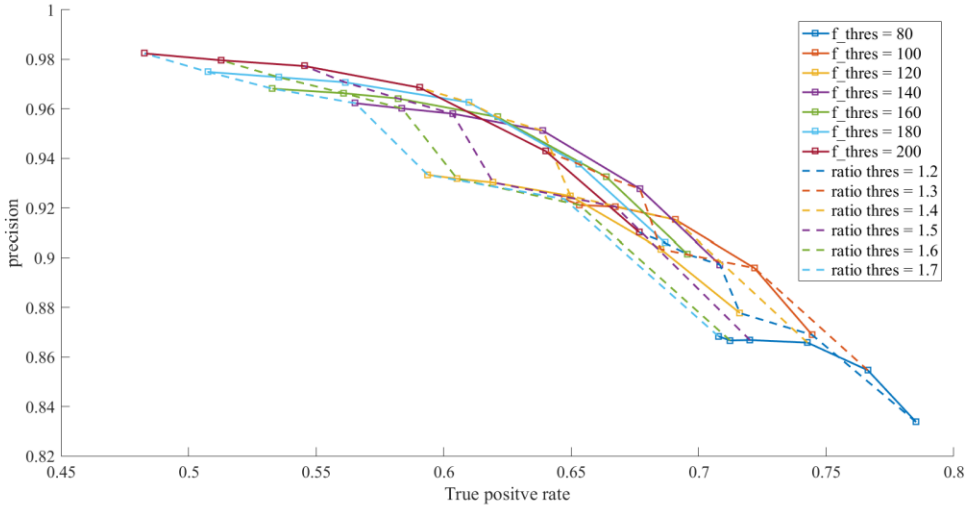

Figure 14 Ali26 Sensitivity vs Accuracy

CHAPTER 4

DISCUSSION

This thesis centers on the development of a frequency based individual neuron cell segmentation algorithm. The overall goal of the algorithm was to achieve fully automated procedure for individual cell segmentation from wide-field fluorescent imaging. This algorithm improves the accuracy of cell identification and provides a promising tool for further neuroscientific studies of the neural network under investigation. Below, we analyze the possible improvement for current errors including false positive error, false negative error and under-/over-segmentation.

There are two possible explanations for false positive error. First, we assume background noise is white but it can be not. Although system noise is the main noise source, which is usually white, additional experimental confounding factors due to various movement from the recording mice also introduce significant noise. Together, this introduces artifacts into recording. If the sensitivity of the dynamic segmentation is set too high, these artifacts would be regarded as cell pixel. Another explanation is that we could miss out some cells when we manually inspect the truth. During the inspection, images were rescaled to computer's gray range which could make people miss out cells has a low luminance. If so, this algorithm can discover more information than we did.

False negative error, which is also called missing rate, is another measurement to judge the performance of an algorithm. In this study, cells with infrequent firing activity would be falsely classified as background noise. Increasing sensitivity of dynamic segmentation could correct some of this error, but in the meantime, it may increase the false positive error as described above. Including additional image frames to expand the dataset and

increase more firing evidence can be another solution since longer sequence will rise the opportunity of cell firing, which improves the accuracy of the algorithm based on PSD. Although adaptive clustering can potentially improve problems associated with under- and over-segmentation, it is still challenging in areas with high cell density since the boundaries of overlapping cells are vague. It is easy to observe that some cells group together and fire synchronously. In this case, two cells show very similar intensity traces which make it hard to separate in clustering tree and cause under-segmentation. In other extreme case, one targeted cell is tightly surround by a group of cells and they have a strong influence to this cell. For an instance, the halo of neighbor cells on the left side will effect left side of targeted cell only. Vice versa, so the targeted cell will be identified as two cells right in the middle because two side of this cell shows different traces. This is a typical situation that cause over-segmentation. Since our algorithm does not consider any morphological features such as cell shape and texture, combining pattern detection or morphology techniques with our algorithm could be a potential approach to reducing under- and over-segmentation. Besides, refining optical instruments with improved spatial resolution will also help reduce segmentation errors.

CHAPTER 5

CONCLUSION

A new algorithm is introduced in this study to segment individual neurons based on frequency domain features. This automatic procedure relies on power spectrum density (PSD) for potential cell detection and hierarchical clustering for cell separation. The method is built on first collecting an intensity trace $\boldsymbol{x_{i,j}}$ for each pixel in order for frequency domain analysis. After a fast Fourier transform, two PSD thresholding processes (static and dynamic, respectively) were used to detect cells within focus and out-of-focus, respectively. For separating cells from a detected group of potential cells, an adaptive clustering tree with correlation coefficient as distance measurement was used to segment individual cells.

Two real datasets recorded from mice hippocampus were tested for this study. Results show that 75% accuracy can be reached while keeping false positive rate under 10%. This result proved that the algorithm is feasible for automatically segmenting large number of cells in a single image frame even when some of the cells overlap. This algorithm can therefore be a candidate for future neuroscience studies where mega scale datasets are generated during each experiment.

REFERENCES

Chen, T., Wardill, T. J., Sun, Y., Pulver, S. R., Renninger, S. L., Baohan, A., … Kim, D. S. (2013). Ultra-sensitive fluorescent proteins for imaging neuronal activity, *499*(7458), 295–300.

Liu, T., Jurrus, E., Seyedhosseini, M., Ellisman, M., & Tasdizen, T. (2012). Watershed Merge Tree Classification for Electron Microscopy Image Segmentation, (Icpr), 133–136.

Meijering, E. (2012). Cell Segmentation : 50 Years Down the Road, (September).

Mohammed, A. I., Gritton, H. J., Tseng, H., Bucklin, M. E., & Yao, Z. (2016). An integrative approach for analyzing hundreds of neurons in task performing mice using wide-field calcium imaging. *Scientific Reports*, *6*(August 2015), 1–16.

Sun, X. R., Badura, A., Pacheco, D. A., Lynch, L. A., Schneider, E. R., Taylor, M. P., … Wang, S. S.-H. (2013). Fast GCaMPs for improved tracking of neuronal activity. *Nature Communications*, *4*, 1–10.

Tian, L., Hires, S. A., Mao, T., Huber, D., Chiappe, M. E., Chalasani, S. H., … Looger, L. L. (2009). Imaging neural activity in worms, flies and mice with improved GCaMP calcium indicators. *Nature Methods*, *6*(12), 875–881. http://doi.org/10.1038/nmeth.1398

Wu, H., & Barbat, J. (1996). An iterative algorithm for cell segmentation using short-time Fourier transform, *184*(November), 127–132.